MOLECULAR ECOLOGY

Molecular Ecology (2011) **20**, 3014–3026 doi: 10.1111/j.1365-294X.2011.05144.x

Molecular evidence for Pleistocene refugia at the eastern edge of the Tibetan Plateau

XIANGJIANG ZHAN,*†[1] YIFANG ZHENG,*‡[1] FUWEN WEI,* MICHAEL W. BRUFORD†[2] and CHENXI JIA*[2]

*Key Lab of Animal Ecology and Conservation Biology, Institute of Zoology, Chinese Academy of Sciences, 1-5 Beichenxi Road, Chaoyang, Beijing 100101, China, †Organisms and Environment Division, Cardiff School of Biosciences, Cardiff University, Cardiff CF10 3AX, UK, ‡Graduate School of Chinese Academy of Sciences, Beijing 100039, China

Abstract

The role of the Quaternary ice ages in forming the contemporary genetic structure of populations has been well studied in a number of global regions. However, due to the different nature of glaciations and complex topography, their role in shaping eastern Eurasian genetic diversity, particular in areas surrounding the Tibetan Plateau have remained largely unstudied. We aimed to address this question by examining the genetic structure of an alpine forest-associated taxon, the blood pheasant (*Ithaginis cruentus*) to infer its phylogeographic history. We detected three phylogenetic lineages and four current population groups. By comparing molecular and palaeovegetation data, we found that major glaciations during the Pleistocene have had a major impact upon the current genetic diversity of this species. Coalescent simulations indicate that the populations retreated to different refugia during some glacial periods in the Pleistocene, but persisted through the last glacial maximum (LGM). The most significant recent population expansion was found to have occurred before the LGM, during which palaeoclimatic data indicate that the climate was both warmer and wetter than today. In contrast, during the LGM populations may have adopted an altitudinal shift strategy in order to track changes in alpine glaciers, exemplifying a general response for montane species in the region where alpine glaciations were not large enough to cause qualitative changes in vegetation. Although analysis based on a plumage related gene showed that divergent selection may have contributed to current patterns of intra-specific diversity, demographic isolation is inferred to have played a more dominant role.

Keywords: blood pheasant, glaciation, Pleistocene refugia, Tibetan Plateau

Received 6 February 2011; revision received 20 April 2011; accepted 28 April 2011

Introduction

Molecular phylogeographic studies have greatly informed evolutionary biology in recent decades (Avise 2000) and have shown that the Quaternary ice ages played a major role in forming the contemporary diversity of many populations, species and communities across the globe (Hewitt 2000). For example, in western Eurasia, during glacial episodes (dry and/or cold), species retreated southwards to climatic refugia (e.g. the Balkans, Italian and Spanish peninsulae; Hewitt 2000) and, after subsequent warming, expanded northwards, dispersing into their current distribution areas. In eastern Eurasia, however, there was no large-scale continental glaciation during the Quaternary. Instead, the uplift of the Tibetan Plateau before the Pleistocene (Wang *et al*. 2008) has produced a complex topography in the region, resulting in a network of high mountains and deep valleys. As a consequence, relatively small alpine glaciers were formed in the Tibetan plateau and its

Correspondence: Chenxi Jia, Fax: +86 10 64807099;
E-mail: jiacx@ioz.ac.cn
Michael W. Bruford, Fax:+44 0 29 208 74116;
E-mail: brufordmw@cf.ac.uk
[1]These two authors contributed equally to the paper.
[2]These two authors are joint senior authors.

surrounds (Chen 1984; Xia 1997). Therefore, in this region more complex glacial effects are expected to have influenced biotic distribution than, for example, in Europe.

To date however, although a number of species have been studied (Zhang *et al.* 2005; Chen *et al.* 2008; Wang *et al.* 2009; Yang *et al.* 2009), the influence of Quaternary glaciations on the Tibetan Plateau, for example, the location of refugia, species' responses to geological events, and the process of postglacial colonization, remain poorly understood. First, while some studies of endemic plants (Zhang *et al.* 2005; Chen *et al.* 2008; but Wang *et al.* 2009) and 'plateau platform' birds (Qu *et al.* 2010) have suggested a possible refugium along the eastern margin of Tibetan Plateau, others, especially avian studies, have failed to detect evidence for glacial refugia for 'edge' species distributed in this region (Qu *et al.* 2010), and little population genetic structure has been found. Second, although a variety of postglacial scenarios have been speculated for species on the Tibetan Plateau (Yang *et al.* 2009), to date, there is scant evidence showing postglacial colonization routes.

One major reason for this lack of resolution could be the different nature of glaciations in this region. Unlike the large-scale movements of species affected by continental-scale glaciations, alpine events allow for altitudinal shifts or minor range changes (Hewitt 2000). Hence, the 'leading edge' model of leptokurtic dispersal and colonization found in regions under major glaciations (Hewitt 1993), has been found to be insufficient in interpreting more complex patterns. A second reason is that previous work in the region has not used detailed palaeoclimate and palaeovegetation data, and interpretation of patterns based in the context of current habitats is problematic. Here, we present an integrated analysis of a common, forest dependent taxon using genetic and key palaeo-data to reveal evidence for glacial refugia on the east edge of the Tibetan Plateau, a region that includes two of 34 global biodiversity hotspots (http://www.biodiversityhotspots.org).

The blood pheasant is mainly distributed on the eastern edge of the plateau, the Qinling Mountains (Mts.) and southern Himalayas, including Sikkim, Burma and Nepal (Yang *et al.* 1994; Fig. 1). Blood pheasants generally prefer coniferous or mixed forests and scrub areas at the snowline, and actively respond to temperature fluctuations, especially heavy snowfall. In summer, blood pheasants breed in montane coniferous forests up to 4600 m (Johnsgard 1999), but migrate in winter to lower elevations (*c.* 1700 m, Cheng 1978). Its wide distribution and active reaction to climatic oscillations make the blood pheasant an ideal organism to reflect the relationship between species distribution and historical climatic factors on the eastern Tibetan Plateau. The blood pheasant also shows evidence of localized population differentiation. Its morphology is sufficiently diverse that large and varying numbers of subspecies have been proposed (Cheng 1978; Johnsgard 1999). Further, there are some more general morphological differences such as the wing colour, from which some taxonomists have classified just two plumage groups, that is, the red-winged and green-winged blood pheasants (Cheng 1978; Johnsgard 1999).

In this study, we used both mitochondrial (mt) and nuclear (n) DNA sequences to study the blood pheasant across its range, and tested hypotheses regarding historical population processes. By comparing molecular data with palaeovegetational evidence provided mainly by

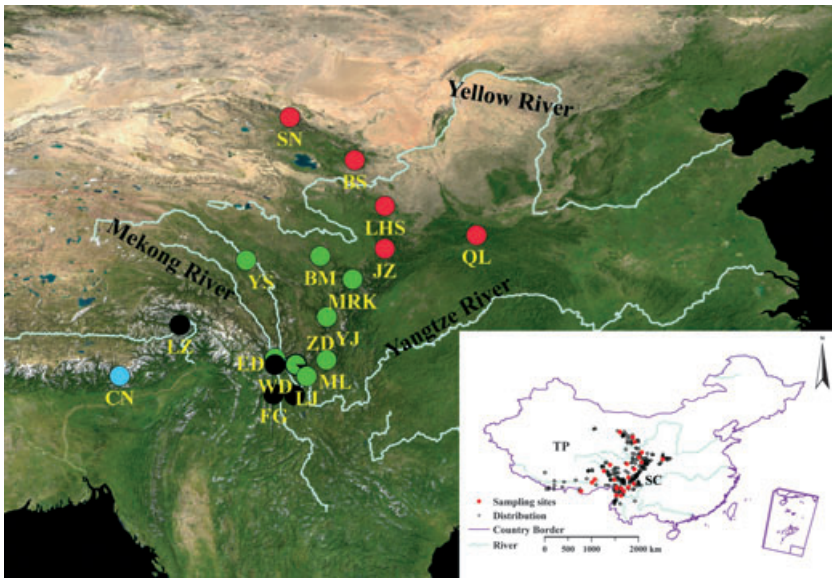

Fig. 1 Sampling sites and haplogroups (HPGs) of pheasant populations superimposed on the map of China using ArcGIS version 9.2 (ESRI): red, HPG A; light green, HPG B; black, HPG C; blue, Population CN. Inset: recorded distribution sites of the blood pheasant in China (Zhang & Ding 2007) and sampling sites in this study. TP: Tibetan Plateau; SC: Sichuan Basin.

pollen cores, we reconstructed an evolutionary hypothesis for the history of this species in the Tibetan Plateau. We further analysed data from the melanin-pathway gene *MC1R* (melanocortin-1-receptor), because it is in some cases related to plumage colour variation in birds (e.g. Mundy 2005; Hull *et al.* 2010). By analyzing *MC1R*, we aimed to test whether a signal of local divergent selection could be overlaid on the demographic evidence accumulated from the mitochondrial and other nuclear data.

The overall aims of this study were (i) to examine the molecular data produced for this endemic alpine forest-associated bird to establish whether it possesses signatures of isolation and subsequent demographic expansion typical of a species confined to one or more glacial refugia during the recent past and (ii) to compare these results with taxonomically relevant morphological characters to assess the relative influence of selection on the phenotypic diversity seen across the range today.

Materials and methods

Study area and sampling

Ten of eleven subspecies described by Johnsgard (1999) were sampled from 23 sites around the Tibetan Plateau (Fig. 1, Table S1, Supporting information). In some sites, samples were purposefully collected from either side of major potential dispersal barriers such as the Mekong River, to examine their correlation with genetic structure. In total, 290 samples (muscle, blood and feathers) were used. 130 muscle samples were from specimens confiscated by local forestry administrations and 47 blood samples from radio-collared pheasants. Once collected, the tissue samples were stored in tubes with 99.7% ethanol. 113 feathers were also collected, sealed in paper bags and stored in silica gel desiccators at room temperature.

DNA extraction, amplification and sequencing

Total DNA from tissues and feathers were extracted using standard Phenol–Chloroform methods (Sambrook *et al.* 1989) and the TIANamp Micro DNA kit (Tiangen), respectively. As shown in Table S2 (Supporting information), the primer pairs, L15164 & H16065, PHDL & PHDH, 00132F & R, 01580F & R, 13380F & R, MSHR72 & 9 were respectively used to amplify mitochondrial *cyt b* (*cytochrome b*) and *cr* (*control region*), the nuclear ENS00132, ENS01580, ENS13380 (Backström *et al.* 2008), and the *MC1R* gene. Detailed PCR information is shown in the Data S1 (Supporting information). PCR products were sequenced using the original amplification primers and, in some cases, internal primers (Table S2, Supporting information) and electrophoresed on a 3130XL Genetic Analyser (Applied Biosystems).

MtDNA phylogenetics and diversity estimation

All sequences were eye-checked, edited and then aligned using CLUSTALW in MEGA4.1 (Tamura *et al.* 2007). To avoid amplifying mitochondrial DNA homologues from the nuclear genome, we blasted the sequences in GenBank and verified the sequences following Zhan & Zhang (2005). For mitochondrial *cyt b* and *cr*, we concatenated the two segments where possible and used the combined sequences for the following analyses.

Phylogenetic relationships among mtDNA haplotypes were estimated using a maximum-likelihood (ML) tree constructed using aLRT–PHYML (Guindon & Gascuel 2003). The best-fit model of nucleotide substitution was chosen by jMODELTEST (Posada 2008) and the topology of the tree was optimized, rather than the branch length. We used the approximate likelihood ratio test (aLRT; Anisimova & Gascuel 2006) with the Shimodaira–Hasegawa-like procedure option to estimate the reliability of each node. A caveat in these analyses is that some phylogenetic assumptions may be violated at the population level, for example, the presence of undetected ancestral haplotypes.

Haplotype (*Hd*) and nucleotide (π) diversities were calculated for each phylogenetic group by DNASP version 5.10 (Librado & Rozas 2009). For the population Cona (CN in Table S1, Supporting information), although it was isolated from others geographically (Fig. 1), only two samples were collected, which might greatly bias molecular analysis sensitive to small sample size. Therefore, except for phylogenetic reconstruction, we removed the population from other analyses.

Population analysis

Pairwise genetic differentiation between main population groups was calculated using ARLEQUIN 3.1 (Excoffier *et al.* 2005). Three approaches were used to examine geographic partitioning of genetic diversity. First, a median-joining network based on haplotypes was estimated for each DNA fragment using NETWORK 4.5.1.6 (Bandelt *et al.* 1999). Unphased SNP sites in the nuclear fragments were not considered. Second, Spatial analysis of molecular variance (SAMOVA; Dupanloup *et al.* 2002) was used to infer mitochondrial groups within the studied populations. The method used a simulated annealing procedure to maximize the proportion of total genetic variance due to difference between groups of populations. Third, mitochondrial genetic distances (Φ_{pt}) between individuals were displayed on a principal

component analysis (PCA) obtained with GENALEX6.2 (Peakall & Smouse 2006).

MtDNA historical demography

To estimate the time to most recent common ancestor (TMRCA), we adopted a coalescent-based approach to analyse mtDNA sequences using BEAST (Drummond & Rambaut 2007). In the galliformes there is only one substitution rate (μ) for mitochondrial genes that has been calibrated by fossils, that is, 1.19% per million years (Myr) per lineage for *cyt b* (Weir & Schluter 2008). By comparing the pairwise genetic distances among 189 individuals in our data set using GENALEX6.2, we found the divergences among *cyt b + cr* sequences were generally 1.419 times of those of *cyt b* sequences (Fig. S1, Supporting information), so we assumed a rate of *cyt b + cr* of 1.69% per Myr.

BEAST analyses were performed using five Markov Chain Monte Carlo (MCMC) runs for 40 million iterations, sampling the genealogy and population size parameters every 1000 iterations and discarding the first 10% as burn-in. The HKY + I + G evolutionary model was selected as above and with the prior set at constant size. Although the mean substitution rate was fixed by assuming a calibrated molecular clock, we used an uncorrelated lognormal model (Drummond *et al.* 2006) to account for rate variation among lineages. The mean TMRCA was obtained in TRACER version 1.3 (Rambaut & Drummond 2007) and its reliability was evaluated by the effective sample size (ESS).

We traced population growth using Tajima's D and Fu's F_S estimated by DNASP version 5.10 (Tajima 1989; Fu 1997); Chakraborty's test (Chakraborty 1990) implemented in ARLEQUIN; and by mismatch analysis based on the spatial and sudden expansion models in ARLEQUIN (Rogers & Harpending 1992; Schneider & Excoffier 1999). For a population undergoing exponential growth, its mismatch distribution should fit a unimodal curve. The validity of the model was tested by obtaining the sum of squared differences (SSD) between the observed and estimated mismatch distribution. Finally, a coalescent-based method implemented in FLUCTUATE 1.4 (Kuhner *et al.* 1998) was used to estimate the exponential growth rate (g) for each population group as follows: 10 short chains of 4000 steps were used and five long chains of 400 000 steps, sampling every 20th step; empirical nucleotide frequencies were used; initial g value of 0.0, starting θ_W from Watterson's estimate (Watterson 1975); transition/transversion (*ti/tv*) rates were estimated in jMODELTEST for each groups separately. Runs were repeated three times to ensure consistency of estimates. As the estimates of g are upwardly biased (Kuhner *et al.* 1998), a conservative approach (Zhao *et al.* 2008) was adopted with values larger than three standard deviations (SD) of g regarded as significant.

The time of population expansions (t, time in generations) was calculated through the relationship $\tau = 2ut$ (Rogers & Harpending 1992), where τ was the mode of the mismatch distribution, u is the substitution rate per generation for the whole sequence under study considering that $u = \mu gk$ (k is the number of nucleotides; μ is 1.69% per Myr as above). We assumed 2.5 years as the generation time (T). The T here was calculated as $T = \alpha + [s/(1 - s)]$ (Sæther *et al.* 2005); where s is the expected adult survival rate. Since there is no s-value reported for the blood pheasant, we took the average value (0.595) from eight galliforme species (see Table S3, Supporting information). Age at maturity α refers to the age at which regular breeding of females first occurs and is at age 1 for the blood pheasant (Johnsgard 1999).

nDNA population structure

Based on the population distribution and the mtDNA network (see Results section), we randomly selected 31 samples for nuclear analyses (Fig. S2, Supporting information). We used the program PHASE version 2.1 (Stephens *et al.* 2001; Stephens & Scheet 2005) to reconstruct nuclear haplotypes from population SNP genotype data (Stephens *et al.* 2001; Niu *et al.* 2002). We set the number of iterations as 1000, with a burn-in period of 1000 and ran the simulation five times to get consistent results. Other settings were in default.

Since the nuclear genes chosen are located in different chromosomes in the chicken genome, we analysed each gene separately and constructed four ML trees and four networks using aLRT–PHYML and NETWORK, respectively.

Coalescent analyses and simulation

Statistical phylogeography using coalescent simulations was adopted to test the fit of the observed gene trees to different phylogeographic hypotheses (Richards *et al.* 2007). We divided the samples into several populations based on the PCA analysis. For each simulation, MESQUITE 2.72 (Maddison & Maddison 2009) was used to simulate 100 coalescent mitochondrial genealogies constrained within different population history predefined by the hypotheses tested. Then, DNA sequences were simulated with the same parameters as our actual mtDNA data for each genealogy on each of the replicate gene trees with the optimal evolutionary model selected by jMODELTEST and a generation time of 2.5 years. We used PAUP* 4.0b10 (Swofford 2002) to reconstruct trees from the simulated gene matrices, and

the test statistic *s* (the minimum number of sorting events corresponding to population membership; Slatkin & Maddison 1989) for these trees were calculated. We tested whether the observed genealogies were consistent with the given hypotheses by comparing the *s* of the empirical ML genealogy with those of the simulated genealogies.

Effective population size (*Ne*) for all the simulations was estimated using the mutation parameter θ (*Theta-W*) calculated by DNASP. *Ne* was converted from *Theta* using the equation $\theta = 2\ Nef\mu$ with μ = 4.225 E-8 (1.69% E-8 × 2.5). To conduct the simulations, we set the overall *Ne* to equal the empirical estimate and constrained ancestral *Ne* of the refugial population to a size proportional to the overall *Ne*. TMRCA dates estimated from BEAST were used to construct multiple refugia hypotheses (detailed in Results).

Refugia localization

Based on the most likely population history inferred above, refugia localization reconstruction (RLR; Déparaz *et al.* 2008) was used to locate refugia for each major mtDNA group. The approach, taking phylogenetic and coalescent uncertainty into account, is to examine the probability that each locality has harboured the MRCA (most recent common ancestor) of the clade.

Following Déparaz *et al.* (2008), we first used BEAST to produced 1000 mtDNA genealogies for each major clade by MCMC after convergence. The programme was run for 20 million iterations, sampling the genealogy and population size parameters every 1000 iterations and discarding the first 10% as burn-in. The optimal evolutionary model was selected for each clade using jMODELTEST. We then treated the sampling locality as a character of the individual and reconstructed for each node the state of the 'locality' character in an unordered parsimonious fashion, on the grounds that the blood pheasant has limited dispersal ability (Jia 1996). A tree was counted as having a state at the root (MRCA) if the state is within the optimal set. Then, dividing the final sum of optimal counts by the number of genealogies checked (1000 here) gave a relative score for each sampling site. All of the calculations were performed in MESQUITE. Furthermore, sampling sites with a score more than expected by chance were highlighted by comparing with the expectations simulated under a broken-stick model using PAST (Hammer *et al.* 2001).

Pollen data, palaeovegetation and palaeoclimate reconstruction

Palaeovegetational ranges in the late Pliocene and early Pleistocene were derived from Wang & Xu (1985), Tong *et al.* (1992) and Tang & Shen (1996), while those during the period 30 000–40 000 years ago were reconstructed based on previous pollen work by Tang *et al.* (1998), Shi *et al.* (2001), and Yu *et al.* (2007). The present vegetational distribution of China followed the classifications of the Editorial Committee of Vegetation Atlas of China (2001).

To further explore palaeoclimatic scenarios, we incorporated Chinese loess deposit data spanning the late Pliocene and Pleistocene. Since it is believed that the sequence of palaeosol and loess units provides a proxy record of climatic change comparable to that of ocean sediments (Rutter 1992), much research has been carried out on the Loess Plateau in China in recent years and has found that rates of dust accumulation are small and large, respectively, during periods of summer monsoon dominance (interglacials) and corresponding strengthening of winter monsoon (glaciations; Kemp & Derbyshire 1998). The mass accumulation rate (MAR) data of Chinese loess were downloaded from the World Data Center for Palaeoclimatology (Sun & An 2006). The two study sites for the loess analysis were Zhaojiachuan and Lingtai, which were about 200 km north of the studied blood pheasant population in the Qinling Mts.

Results

Phylogenetic structure

Fifty-nine mtDNA haplotypes (exc. Population CN; see the Data S2, Supporting information) clustered into three major haplogroups (HPGs) in the network analysis (Fig. 1), with 69 substitutions inferred between A and B and 41 between B and C. HPG A comprised sequences from five sampling localities in the north of the studied region (in red in Fig. 1). HPG B included all but one individual (n = 101) sampled from the eight localities in the central region (light green). HPG C included four sites in the southwest (black), as well as one individual from the population ZD in the central (Fig. 1).

Individuals for nDNA sequencing were selected to represent genetic lineages identified from mtDNA analysis (i.e. 9, 10 and 10 for each HPG; Fig. S2, Supporting information). Two nDNA networks supported the distinctiveness of HPG A but not the other two (Fig S5, Supporting information), which may be due to the lower evolutionary rates of nuclear sequences in comparison to the timescales involved (inferred to be <3 Myr from mtDNA, see below). Moreover, ML phylogenies constructed from both mtDNA (Fig. S3, Supporting information) and nDNA (Fig. S4, Supporting information) showed similar patterns as the networks and confirmed that population CN, located south of the

Himalayas, was highly distinct from other clades (see Data S2, Supporting information).

SAMOVA based on mtDNA sequences produced similar significant Φ_{CT} values when numbers of population groups were assumed to be from three to seven (Table S5, Supporting information). But the variable number of populations sampled per group (which was as low as one) could have influenced these results. In this case, the PCA analysis provides an alternative when examining the geographic partitioning of genetic variance (Palmé *et al.* 2003). In the PCA plot, the first and second component produced the same results as in the networks (Fig. 2) and separated the samples into three groups. Further, the third component separated the northern populations into two groups (Fig. S6, Supporting information). These four population groups are denoted as 'North', 'QL', 'Southeast', 'Southwest' according to their relative positions around the Tibetan Plateau (Fig. 1). In the northeast, the 'North' group ranges from SN to JZ and 'QL' is restricted to the Qinling Mts. In the east, 'Southeast' occupies the eastern edge of the plateau. In the southwest, 'Southwest' is distributed in the southern edge of the plateau.

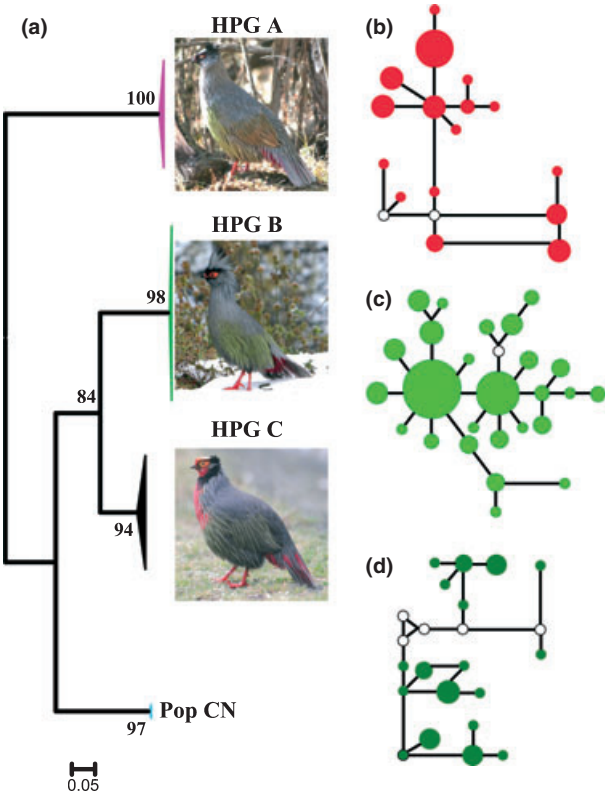

Fig. 2 Maximum-likelihood phylogenetic tree of blood pheasant populations with representative images (a) and mtDNA network for each haplogroup (b–d). The node size is in proportion to the frequency of corresponding haplotype in the whole data set with the smallest equal to one observation. All the lines were drawn according to the number of mutations between neighbouring haplotypes with the shortest equal to one mutation. The hollow circle indicates where an assumed intermediate haplotype was not sampled.

In the population ZD, all except one individual clustered into the Southeastern group. The exceptional individual possessed a distinct Southwestern haplotype and two individuals from the Southwest possessed the same haplotype. Recent immigration could produce this pattern since ZD is located within a contact zone between the two groups (Fig. 1). Also, local people have traditionally hunted blood pheasants in this region, which could include translocation of individuals. We therefore conducted the analysis assuming the lineages assort completely with geographic zone, and removed this individual however it remains possible that occasional natural immigration occurs.

The population structure reflected by *MC1R* sequences was similar to the other nDNA loci and the distribution of the two *MC1R* clades was consistent with the two distinct plumage groups in the species (Fig. S5D, Supporting information). However, although there was one fixed SNP (single-nucleotide polymorphism) between the two groups, it was synonymous and there was no additional evidence of selection acting at this locus.

Divergence time and population expansion

Analyses using BEAST (Table S6, Supporting information) indicated two main divergence events within the blood pheasant: the first occurred 2.49 Myr before present (BP) between the populations in the north (North + QL) and south (Southeast + Southwest), and the second 1.20 Myr between Southeast and Southwest. For each of the four population groups, TMRCA ranged from 0.27 to 0.06 Myr. The significant nonzero distribution of the standard deviation of the relaxed clock (ucld.stedev = 0.835) indicated there is among branch rate heterogeneity in our data set. When including the sample ZD29 for estimating the TMRCA of Southeast group, the inclusion of just this one individual advanced the time by about one Myr, indicating again that it is unlikely that ZD29 originated from the Southeast.

Among the four population groups, two (QL and Southeast) featured unimodal mismatch distributions (Fig. S7, Supporting information) and none deviated significantly from expectation under a model of population expansion (SSD test) regardless of the model used ($P > 0.05$). A significant recent population expansion was detected in the 'Southeast' group in that it recorded significantly negative Tajima's *D*, Fu's *Fs*, significant Chakraborty's values ($P < 0.01$), and significant population growth suggested by the Fluctuate analysis

(g = 1598.614; SD = 214.43). But for other groups, *D* and/or *Fs* were negative but not significant, and all the results of Charkraborty's values and Fluctuate g were nonsignificant (Table S4, Supporting information). According to the mismatch distribution, the time of demographic expansion for each group varied between 246 000 and 21 000 years ago (Table S4, Supporting information).

Phylogeographic hypotheses testing and refugia localization

Based on the empirical θ values, the effective population size for each lineage was derived (Table S6, Supporting information). Three hypotheses concerning the glacial refugia of the blood pheasants were tested (Fig. 3). (i) *Single refugium in the last glacial maximum* (*LGM*): extant populations of the blood pheasant were derived from a single refugium located either in the north (North + QL) or the south (Southeast + Southwest), and the population began to expand as the glaciers retreated at the end of the LGM (*c*. 12 000 years BP; Fig. 3a); (ii) *Single refugium in the middle Pleistocene*: extant populations were from a single refugium located in the north/south, and the population began to expand after the Naynayxungla Glaciations (*c*. 0.6 Myr BP; Fig. 3a); (iii) *Multiple refugia*: the two main lineages split at the beginning of the Pleistocene (*c*. 2.49 Myr BP); with the southern lineage diverging into two further clades 1.20 Myr BP and with the northern branch persisting throughout the Pleistocene finally separating into two populations (*c*. 0.44 Myr BP; Fig. 3b).

From the mitochondrial ML tree, we found that the Slatkin & Maddison's *s* was equal to 28. Then, we calculated the *s*-values for trees constructed from genealogies simulated under different historical hypotheses. The simulation results rejected the single refugium hypotheses at either the LGM or middle Pleistocene ($P < 0.01$). However, the *s*-value of the simulated trees did not reject the multiple refugia hypothesis ($P = 0.29$).

Among the four refugia proposed, 'QL' is the only one that comprises a single, easily defined sampling region (Qinling Mts.), where one could reasonably expect a single regional population might have survived *in situ*. For the others, we used a RLR method to infer refugial locations for each mtDNA group. Our analysis indicated that the three lineages were most likely to have coalesced in different geographic regions. For the 'North' group, this is likely to have been the Lianhuashan Mts. (LHS; Fig 1) because the highest probability (97.7%) was found to be at that sampling site by RLR analysis and this probability was higher than expected by chance when examined using a broken-stick model. For the 'Southeast', three closely spaced sampling sites within the region of the southeastern edge of Tibetan Plateau were similarly implicated with the following probabilities ML (44.83), ZD (27.9), and LJ (23.06), and for the 'Southwest', it was FG (80.11). However, we cannot fully rule out the possibility that a correlation between sample size and probability of a site being an origin population could partially explain the results (Table S1, Supporting information).

Discussion

Four significant glaciations are recognized to have occurred in the Tibetan Plateau during the Pleistocene, the Xixiabangma (Early Pleistocene), Nyanyaxungla (Middle Pleistocene), Guxiang (late Middle Pleistocene) and the last glaciation, including two glacial stages and

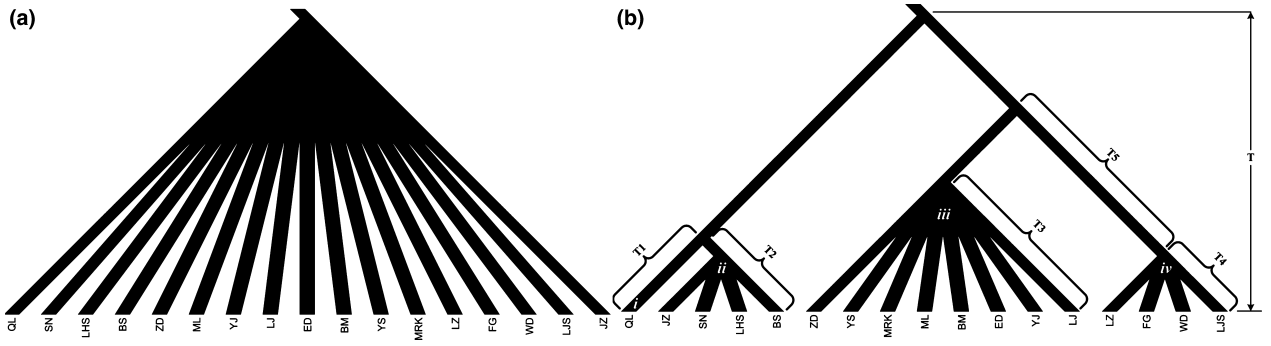

Fig. 3 Models used to test Pleistocene refugial hypotheses: (a) single refugium hypothesis: populations are derived from a single refugium located either in the north (North + QL) or south (Southeast + Southwest), and began to expand at the end of the last glacial maximum (*c*. 12 000 years BP, 4800 *generations (g)*; Hyp 1) or in the middle Pleistocene (*c*. 0.6 Myr BP, 240 000 *g*; Hyp 2). (b) Multiple refugia hypothesis (Hyp 3): two lineages split at the Early Pleistocence (T = 2.49 Myr BP; 1 000 000 *g*); the southern branch diverged into two clades at 480 000 *g* ago (T4 + T5); the north branch persisted throughout most of the Pleistocene but was separated into two populations in the Late Pleistocene. T1–T4 (i.e. 176 000 *g*; 104 000 *g*; 84 000 g; 108 000 *g*) were derived from the estimates based on mtDNA analysis (Table S6, Supporting information), and *i* to *iv* was set to be in proportion to *Ne*.

the last corresponding to the LGM (Shi 2002; Zheng *et al.* 2002). In contrast to previous work (e.g. Qu *et al.* 2010), our coalescent simulations uncovered evidence for at least four Pleistocene refugia affecting genetic structure in the blood pheasant (Fig. 3b). Molecular analysis suggests that, while the common ancestor of the extant populations dated to the Early Pleistocene, three refugial populations were found in the Middle Pleistocene and one in Late Pleistocene. The location of the four refugia could be inferred to different mountain regions within the study area, namely, the Qinling (for the QL) and Lianhuashan (North) in the north-east of Tibetan Plateau, the Muli, Zhongdian, and Lijiang (Southeast) and the Fugong (Southwest; Fig. 1). Additionally, considering its mtDNA distinctiveness (Fig. 2), CN (Table S1, Supporting information) could represent another refugium in the south of the Himalayas because the population extends westward into Nepal and there is a plumage gradient along the southern Himalayas, indicating another possible phylogenetic split. More sampling from that region could help to elucidate the issue.

Recently, pollen cores have been extracted in the Tibetan Plateau and adjacent mountains, which make it possible to infer palaeovegetational changes and their likely influence on the blood pheasant, a species which requires upper montane conifer forest and subalpine shrub (Cheng 1987; Fig. 4d). By comparing inferred refugial areas and palaeovegtational data, especially conifer forest, we explored historical scenarios for the blood pheasant and environment changes in the eastern Tibetan Plateau during the Quaternary.

The TMRCA of the blood pheasant dates to approximately 2.5 Myr BP, during the Early Pleistocene (Gibbard & Head 2009). This is earlier than most previous avian studies (e.g. Yang *et al.* 2009; Qu *et al.* 2010), but overlaps, for example, with the Tibetan Gazelle (*Procapra picticaudata*, Zhang & Jiang 2006) and several other

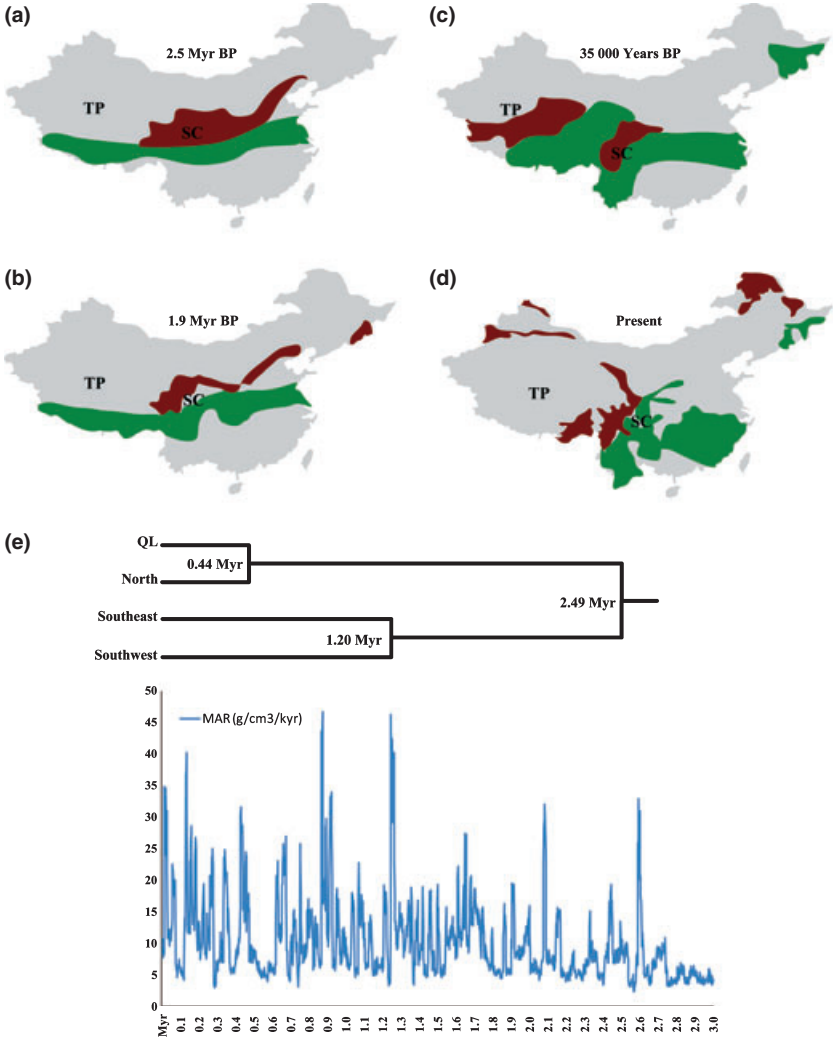

Fig. 4 Palaeo- and current distribution of conifer forest (brown) and conifer-broadleaf forest (green) in China and changes in mass accumulation rates (MAR) of Chinese loess in the Late Pliocene-Plaeistocence. Palaeovegetation maps during the glacial (a) and interglacial period (b) in the Early Pleistocene were drawn mainly according to pollen data (Tong *et al.* 1992; Tang & Shen 1996). (c) Palaeovegetation reconstructed from pollen data in the period of 30 000–40 000 years BP (Tang *et al.* 1998; Shi *et al.* 2001; Yu *et al.* 2007). (d) The present distribution of the forest, which is drawn from GIS-based current vegetation of China (Editorial Committee of Vegetation Atlas of China 2001). TP: Tibetan Plateau; SC: Sichuan Basin. (e) Above: the dated BEAST-derived phylogeny with three divergence times indicated; Below: Late Pliocene-Pleistocence (3.0 Myr BP-present) changes in MAR of loess deposits on the Chinese Loess Plateau. The data were derived from Sun & An (2006).

mammals (e.g. Luo *et al.* 2004; Jin *et al.* 2008). Geological studies have shown that the beginning of the Pleistocene was marked by the first Quaternary glacial period in China (Wang & Xu 1985; Tong *et al.* 1992) and Chinese loess data provide consistent evidence because the first accumulation peak formed about 2.6 Myr BP (Fig. 4e). Although the date of the Xixiabangma glaciations remains unresolved (Shi 2002; Zheng *et al.* 2002), we postulate that it may also have been *c.* 2.6 Myr BP based on the available biological and geological evidence. For the blood pheasant, a reconstructed vegetation map using pollen core data (Fig. 4a) shows that two kinds of conifer-bearing forest retreated to the south of the Tibetan Plateau, Sichuan Basin and parts of central China, implying that the first refugium for the blood pheasant was located in this region.

In the interstadial of Early Pleistocene, the glaciers retreated, and the climate became warmer and wetter in China, supported by decreased accumulation rates of Chinese loess (Fig. 4e). Accordingly, conifer forest would have expanded northwards (Fig. 4b) such that blood pheasant populations could colonize new suitable habitats. Unexpectedly, pollen core data show that extensive grasslands appeared in the Sichuan Basin, dividing pheasant habitat into two with only the extreme edge connected (Fig. 4b). Therefore, the first intraspecific divergence event within the blood pheasant lineage may have followed vegetation shifts and a period of isolation during the processes of postglacial colonization. The population in the north is therefore inferred to have diverged allopatrically (Fig. 4b) to give rise to the HPG A mitochondrial lineage (i.e. North & QL groups).

Our data suggest that the TMRCA for the Southeast and Southwest groups is approximately 1.2 Myr BP. This date coincides with another cold stage in the Xixiabangma glaciations (Zheng *et al.* 2002) and a high MAR for Chinese loess supports that it is one of coldest recent climatic periods in the region (Fig. 4e), possibly creating a refugium in the south. In contrast, the northern populations seem to have been unaffected by this glacial period instead retreating into a refugium during the following glaciation (Naynayxungla, *c.* 0.5 Myr BP), coinciding with another MAR peak of Chinese loess (Fig. 4e).

In the late Middle Pleistocene, corresponding to the Guxiang glacial period, the largest glaciations occurred along the eastern edge of Tibetan Plateau and valley glaciers were highly developed (Zheng *et al.* 2002). During this harsh climatic period, we infer three refugia for the blood pheasant, localized to Lianhuashan for the North group, Muli, Lijiang and Zhongdian for the Southeast and Fugong for the Southwest. Another refugium is inferred to be Qinling for the QL group around 0.06 Myr BP, during the early stage of the last glaciation in the plateau ('Taibai Glacial I' in the Qinling area). In contrast, during the LGM (around 18 000 years ago), it seems that all four groups persisted. That little effect of LGM on the populations is a distinct regional feature compared to Europe and North America (Beatty & Provan 2010), but evidence is accumulating that it is relatively common for species in China (e.g. Li *et al.* 2009; Qu *et al.* 2010).

Among the four population groups, two possessed signals of recent growth (Fig. S7 and Table S4, Supporting information). The Southeast group was estimated to have expanded at about 40 000 years ago, earlier than the LGM and is likely to be the consequence of the warm and wet climate during that period, usually referred to as the 'Greatest Lake Period' in China (30 000–40 000 years ago; Shi *et al.* 2001; Yu *et al.* 2007). ^{18}O analysis of ice cores from the Tibetan Plateau suggests that the temperature was 2–4 °C higher and precipitation was 40–100% higher than today (Shi *et al.* 2001). Furthermore, pollen-based vegetation reconstruction shows that at this time (Fig. 4c; Tang *et al.* 1998; Yu *et al.* 2007), the alpine conifer forest extended *c.* 400–800 km beyond its present western limit (Fig. 4d).

The most recent expansions of the QL group is inferred to have happened after the LGM. It is recorded that a significant alpine glacier, Taibai glacial II, developed in the Qinling Mts. in the LGM (Tian & Huang 1990; Shi 2002). However, in contrast to classical glaciers in Europe and America, even during the LGM, there was conifer forest remaining (Tian & Huang 1990; Harrison *et al.* 2001), and summer precipitation did not differ significantly from its current levels (Ju *et al.* 2007). Thus, blood pheasants in the Qinling may have simply retreated to lower altitudes, a response that could be a general feature in the montane areas around the Tibetan Plateau where alpine glaciations were not large enough to cause qualitative changes in vegetation.

While genetic variation within the blood pheasant was partitioned by mountain ranges, no effect of large rivers could be detected in our study area. The species seems to have expanded across the two largest rivers in China, the Yangtze and Yellow (Fig. 1) and although the populations on different sides of the Mekong River (ED vs. WD) were genetically distinct, LJS in the east side of the same river was found to be genetically closer to the west side and there was a shared haplotype between the two riversides (Fig. 1), suggesting that the Mekong River is also not a dispersal barrier for the blood pheasant.

Blood pheasant taxonomy has been debated and nine to fourteen subspecies have been classified (Delacour 1951; Cheng 1978, 1987; Howard & Moore 1980; Yang *et al.* 1994). Several studies even upgraded some sub-

species to species (Beebe 1990; Wen *et al*. 2009). Our study uncovered significant population genetic structure in the blood pheasant, and found that the molecular pattern detected could be matched to major phenotypic groups (e.g. Fig. 2; Table S7, Supporting information).

Generally, our results support the two plumage groups previously proposed by morphologists (Cheng 1978; Johnsgard 1999) with males in northern populations (Group QL and North) possessing reddish brown as opposed to green wing-coverts or those tinged with green. Interestingly, 'ear-tufts' are distinctive for males and females from northern populations, but are absent or greatly reduced in southern populations. Further, the face and throat of females from localities in the north are grey, while they are reddish brown in regions in the south (Cheng 1978; Johnsgard 1999). Finally, males from the southwest populations generally have a crimson head and breast whereas those from the southeast do not.

For the plumage related gene, *MC1R*, we did find a correlation between the *MC1R* genotype and wing colour in male blood pheasants (Fig. 2 and S5D, Supporting information) with the two major phenotypes possessing a fixed SNP difference. However, most substitutions detected in the gene (including the above example) were synonymous. Moreover, other putatively neutral sequences, especially mitochondrial *cyt b/cr*, showed similar and/or more detailed population structure (Fig. 2) to *MC1R* (Fig. S5D, Supporting information). Therefore, it seems that the sequences used in the present study are not subject to strong divergent selection and the phylogeographic pattern detected here (Fig. 1) is mainly the consequence of historical demographic events.

Our study shows that all the four major glaciations in the Pleistocene have left some imprints on the evolution of the blood pheasant. However, the pattern uncovered in the Tibetan Plateau is very different from that in Europe. No large-scaled retreat was found during the Pleistocene glaciations and only evidence for altitudinal shifts was observed in the species during the relative 'mild' LGM. Furthermore, by exploring historical scenarios of the blood pheasant, we found the large mountain ranges on the Tibetan Plateau, especially those in the east edge, have provided substantial refugia for the species during the Quaternary. Since there are many species sympatrically distributed in the area, we may expect that same geological processes could have similar effects on regional historical demography. These processes, thus, might be the main reason why the east edge of the Tibetan Plateau has generated and maintained one of the most important biodiversity centres in the world.

Acknowledgements

This work was supported by the National Natural Science Foundation of China (30670284 and 30970337) and the Knowledge Innovation Programme of Chinese Academy of Sciences to X.Z. We thank Fan Yang, Yuehua Sun, Huisheng Gong, Shuping Fan, Larongchunzha, Xiamalachu, Yongzhong, Adu, Renzengduojie, Goumujia for their help with fieldwork; Drs Laurent Excoffier, Rasmus Nielson, Wayne Maddison, and Markus Pfenninger for their suggestions on analyzing data; Dr Jian Ni and Mrs Shuixian Fan for their advice on palaeovegetation reconstruction; Miss Chi Chen for her help in refining the figures and Dr Yoshan Moodley for his comments on earlier version the manuscript; X.Z. also thanks Dr Jiang Chang, and Y. Z. thanks Drs Ming Li, Hua Wu, Yibo Hu, and Qiong Zhang for their help in the experiment.

References

Anisimova M, Gascuel O (2006) Approximate likelihood ratio test for branches: a fast, accurate and powerful alternative. *System Biology*, **55**, 539–552.

Avise JC (2000) *Phylogeography: The History and Formation of Species*. Harvard University Press, Cambridge, MA.

Backström N, Fagerberg S, Ellegren H (2008) Genomics of natural bird populations: a gene-based set of reference markers evenly spread across the avian genome. *Molecular Ecology*, **17**, 964–980.

Bandelt HJ, Forster P, Röhl A (1999) Median–joining networks for inferring intraspecific phylogenies. *Molecular Biology and Evolution*, **16**, 37–48.

Beatty GE, Provan J (2010) Refugial persistence and postglacial recolonization of North America by the cold-tolerant herbaceous plant *Orthilia secunda*. *Molecular Ecology*, **19**, 5009–5021.

Beebe W (1990) *A Monograph of the Pheasants*. Dover Publications, London.

Chakraborty R (1990) Mitochondrial DNA polymorphism reveals hidden heterogeneity within some Asian populations. *American Journal of Human Genetics*, **47**, 87–94.

Chen YY (1984) *Geology in the Quaternary*. Hebei Normal University Press, Shijiazhuang, China.

Chen SY, Wu GL, Zhang DJ *et al*. (2008) Potential refugium on the Qinghai-Tibet Plateau revealed by the chloroplast DNA phylogeography of the alpine species *Metagentiana striata* (Gentianaceae). *Botanical Journal of the Linnean Society*, **157**, 125–140.

Cheng TH (1978) *Fauna sinica. Aves. Vol 4: Galliformes*, pp. 182–186. Sciences Press, Beijing.

Cheng TH (1987) *A Synopsis of the Avifauna of China*. Science Press, Beijing.

Delacour J (1951) *The Pheasants of the World*. Country Life Limited, London.

Déparaz A, Codellier M, Hausser J, Pfenninger M (2008) Postglacial recoloniztion at a snail's pace (*Trochulus villosus*): confronting competing refugia hypotheses using model selection. *Molecular Ecology*, **17**, 2449–2462.

Drummond AJ, Ho SYW, Phillips MJ, Rambaut A (2006) Relaxed phylogenetics and dating with confidence. *PLoS Biology*, **4**, e88.

Drummond AJ, Rambaut A (2007) BEAST: Bayesian evolutionary analysis by sampling trees. *BMC Evolutionary Biology*, **7**, 214.

Dupanloup I, Schneiderl S, Excoffier L (2002) A simulated annealing approach to define the genetic structure of populations. *Molecular Ecology*, **11**, 2571–2581.

Editorial Committee of Vegetation Atlas of China, Chinese Academy of Sciences (2001) *Vegetation Atlas of China*. Science Press, Beijing.

Excoffier L, Laval G, Schneider S (2005) Arlequin *v*3.0: an integrated software package for population genetics data analysis. *Evolutionary Bioinformatics Online*, **1**, 47–50.

Fu YX (1997) Statistical tests of neutrality of mutations against population growth, hitchhiking and background selection. *Genetics*, **147**, 915–925.

Gibbard PL, Head MJ (2009) IUGS ratification of the Quaternary system/period and the Pleistocene series/epoch with a base at 2.58MA. *Quaternaire*, **20**, 411–412.

Guindon S, Gascuel O (2003) A simple, fast and accurate method to estimate large phylogenies by maximum-likelihood. *System Biology*, **52**, 696–704.

Hammer Ø, Harper DAT, Ryan PD (2001) PAST: paleontological statistics software package for education and data analysis. *Palaeontologia Electronica*, **4**, 9.

Harrison SP, Yu G, Takahara H, Prentice IC (2001) Palaeovegetation – diversity of temperate plants in east Asia. *Nature*, **413**, 129–130.

Hewitt GM (1993) After the ice: parrellel meets Ethyropus in the Pyrenees. In:*Hybrid Zones and Evolutionary Process* (ed. Harrison RG). pp. 140–164, Oxford University Press, Oxford.

Hewitt GM (2000) The genetic legacy of the quaternary ice ages. *Nature*, **405**, 907–913.

Howard R, Moore A (1980) *A Complete Checklist of the Birds of the World*. Oxford University Press, New York.

Hull JM, Mindell DP, Talbot SL, Kay EH, Hoekstra HE, Ernest HB (2010) Population structure and plumage polymorphism: the intraspecific evolutionary relationships of a polymorphic raptor, *Buteo jamaicensis harlani*. *BMC Evolutionary Biology*, **10**, 224–235.

Jia CX (1996) *Studies on habitat selection, breeding ecology and behaviour of blood pheasant*. PhD Thesis, Beijing Normal University, Beijing.

Jin Y, Brown RP, Liu N (2008) Cladogenesis and phylogeography of the lizard *Phrynocephalus vlangalii* (Agamidae) on the Tibetan plateau. *Molecular Ecology*, **17**, 1971–1982.

Johnsgard PA (1999) *The Pheasants of the World*, 2nd edn. pp. 92–99. Oxford University Press, Oxford.

Ju L, Wang H, Jiang D (2007) Simulation of the Last Glacial Maximum climate over East Asia with a regional climate model nested in a general circulation model. *Palaeogeography, Palaeoclimatology, Palaeoecology*, **248**, 376–390.

Kemp RA, Derbyshire E (1998) The loess soils of China as records of climatic change. *European Journal of Soil Science*, **49**, 525–539.

Kuhner MK, Yamato J, Felsenstein J (1998) Maximum likelihood estimation of population growth rates based on the coalescent. *Genetics*, **149**, 429–434.

Li SH, Yeung CKL, Feinstein J *et al.* (2009) Sailing through the Late Pleistocene: unusual historical demography of an East Asian endemic, the Chinese Hwamei (*Leucodioptron canorum canorum*), during the last glacial period. *Molecular Ecology*, **18**, 622–633.

Librado P, Rozas J (2009) DnaSP *v*5: a software for comprehensive analysis of DNA polymorphism data. *Bioinformatics*, **25**, 1451–1452.

Luo J, Yang DM, Suzuki H *et al.* (2004) Molecular phylogeny and biogeography of Oriental voles: genus *Eothenomys* (Muridae, Mammalia). *Molecular Phylogenetics and Evolution*, **33**, 349–362.

Maddison WP, Maddison DR (2009) Mesquite: a modular system for evolutionary analysis. Version 2.72 http://mesquiteproject.org.

Mundy NI (2005) A window on the genetics of evolution: MC1R and plumage colouration in birds. *Proceedings of the Royal Society of London Series B-Biological Sciences*, **272**, 1633–1640.

Niu T, Qin ZS, Xu X, Liu SJ (2002) Bayesian haplotype inference for multiple linked single-nucleotide polymorphisms. *American Journal of Human Genetics*, **70**, 157–169.

Palmé AE, Su Q, Rautenberg A, Manni F, Lascoux M (2003) Postglacial recolonization and cpDNA variation of silver birch, *Betula pendula*. *Molecular Ecology*, **12**, 201–212.

Peakall R, Smouse PE (2006) GENALEX 6: genetic analysis in Excel. Population genetic software for teaching and research. *Molecular Ecology Notes*, **6**, 288–295.

Posada D (2008) jModelTest: phylogenetic model averaging. *Molecular Biology and Evolution*, **25**, 1253–1256.

Qu Y, Lei F, Zhang R, Lu X (2010) Comparative phylogeography of five avian species: implications for Pleistocene evolutionary history in the Qinghai-Tibetan plateau. *Molecular Ecology*, **19**, 338–351.

Richards CL, Carstens BC, Knowles LL (2007) Distribution modelling and statistical phylogeography: an integrative framework for generating and testing alternative biogeographical hypotheses. *Journal of Biogeography*, **34**, 1833–1845.

Rogers AR, Harpending H (1992) Population growth makes waves in the distribution of pairwise genetic differences. *Molecular Biology and Evolution*, **9**, 552–569.

Rutter N (1992) Presidential address, XIII INQUA Congress 1991: Chinese loess and global change. *Quaternary Science Reviews*, **11**, 275–281.

Sæther BE, Lande R, Engen S *et al.* (2005) Generation time and temporal scaling of bird population dynamics. *Nature*, **436**, 99–102.

Sambrook J, Fritsch EF, Maniatis T (1989) *Molecular Cloning: A Laboratory Manual*, 2nd edn. Cold Spring Harbor Laboratory Press, New York.

Schneider S, Excoffier L (1999) Estimation of demographic parameters from the distribution of pairwise differences when the mutation rates vary among sites: application to human mitochondrial DNA. *Genetics*, **152**, 1079–1089.

Shi YF (2002) A suggestion to improve the chronology of Quaternary glaciations in China. *Journal of Glaciology and Geocryology*, **24**, 687–692.

Shi YF, Yu G, Liu XD, Li BY, Yao TD (2001) Reconstruction for 30–40 Ka B.P. enhanced Indian monsoon based on geological records from the Tibetan Plateau. *Palaeogeography, Palaeoclimatology, Palaeoecology*, **169**, 69–83.

Slatkin M, Maddison WP (1989) A cladistic measure of gene flow inferred from phylogenies of alleles. *Genetics*, **123**, 603–613.

Stephens M, Scheet P (2005) Accounting for decay of linkage disequilibrium in haplotype inference and missing data imputation. *American Journal of Human Genetics*, **76**, 449–462.

Stephens M, Smith NJ, Donnelly P (2001) A new statistical method for haplotype reconstruction from population data. *American Journal of Human Genetics*, **68**, 978–989.

Sun YB, An ZS (2006) Chinese Loess Plateau mass accumulation rate data. IGBP PAGES/World Data Center for Paleoclimatology. Data Contribution Series # 2006-034. NOAA/NCDC Paleoclimatology Programme, Boulder, CO, USA.

Swofford DL (2002) *PAUP*. Phylogenetic Analysis Using Parsimony (*and other methods). Version 4.0b10*. Sinauer Associates, Sunderland, MA.

Tajima F (1989) Statistical method for testing the neutral mutation hypothesis by DNA polymorphism. *Genetics*, **123**, 585–595.

Tamura K, Dudley J, Nei M, Kumar S (2007) MEGA4: Molecular Evolutionary Genetics Analysis (MEGA) software version 4.0. *Molecular Biology and Evolution*, **24**, 1596–1599.

Tang LY, Shen CM (1996) Late cenozoic vegetational history and climatic characteristics of Qinghai-Xizang Plateau. *Acta anaesthesiologica Sinica*, **13**, 321–337.

Tang LY, Shen CM, Kong ZC, Wang FB, Liu KB (1998) Pollen evidence of climate during the last glacial maximum in eastern Tibetan Plateau. *Journal of Glaciology and Geocryology*, **20**, 133–140.

Tian ZS, Huang CC (1990) The glaciations process in Mt. Taibai of the Qinling Mountains and the climatic changes in the Loess Plateau. *Geographical Research*, **9**, 15–23.

Tong GB, Zhang JP, Fan SX (1992) Distribution of Quaternary palynoflora in China. *Marine Geology and Quaternary Geology*, **12**, 45–56.

Wang KF, Xu X (1985) *Quaternary Palynology*. Guizhou People's Press, Guiyang.

Wang CS, Zhao XX, Liu ZF *et al.* (2008) Constraints on the early uplift history of the Tibetan Plateau. *Proceedings of the National Academy of Sciences USA*, **105**, 4987–4992.

Wang LY, Abbott RJ, Zheng W, Chen P, Wang YJ, Liu JQ (2009) History and evolution of alpine plants endemic to the Qinghai-Tibetan Plateau: *Aconitum gymnandrum* (Ranunculaceae). *Molecular Ecology*, **18**, 709–721.

Watterson GA (1975) On the number of segregating sites in genetical models without recombination. *Theoretical Population Biology*, **7**, 256–276.

Weir JT, Schluter D (2008) Calibrating the avian molecular clock. *Molecular Ecology*, **17**, 2321–2328.

Wen LY, Bao XK, Wang LC, Liu NF (2009) Study on the taxonomy and genetic divergence of *Ithaginis*. *Acta Zootaxonomica Sinica*, **34**, 180–183.

Xia ZK (1997) *Environment in the Quaternary*. Beijing University Press, Beijing.

Yang L, Wen JX, Yang XJ (1994) On the taxonomy of blood pheasant (*Ithaginis*). *Zoological Research*, **15**, 21–30.

Yang SJ, Dong HL, Lei FM (2009) Phylogeography of regional fauna on the Tibetan Plateau: a review. *Progress in Natural Science*, **19**, 789–799.

Yu G, Gui F, Shi YF, Zheng YQ (2007) Late marine isotope stage 3 palaeoclimate for East Asia: a data-model comparison. *Palaeogeography, Palaeoclimatology, Palaeoecology*, **250**, 167–183.

Zhan XJ, Zhang ZW (2005) Molecular phylogeny of avian genus *Syrmaticus* based on the mitochondrial *cytochrome b* gene and control region. *Zoological Sciences*, **22**, 427–435.

Zhang CA, Ding CQ (2007) The site record database for Chinese galliformes and its application. *Chinese Journal of Zoology*, **42**, 73–78.

Zhang FF, Jiang ZG (2006) Mitochondrial phylogeography and genetic diversity of Tibetan gazelle (*Procapra picticaudata*): implication for conservation. *Molecular Phylogenetics and Evolution*, **41**, 313–321.

Zhang Q, Chiang TY, George M, Liu JQ, Abbott RJ (2005) Phylogeography of the Qinghai-Tibetan Plateau endemic *Juniperus przewalskii* (Cupressaceae) inferred from chloroplast DNA sequence variation. *Molecular Ecology*, **14**, 3513–3524.

Zhao L, Zhang J, Liu ZJ *et al.* (2008) Complex population genetic and demographic history of the Salangid, *Neosalanx taihuensis*, based on cytochrome b sequences. *BMC Evolutionary Biology*, **8**, 201.

Zheng BX, Xu QQ, Shen YP (2002) The relationship between climate change and Quaternary glacial cycles on the Qinghai–Tibetan Plateau: review and speculation. *Quaternary International*, **97–98**, 93–101.

The laboratory of CX Jia at the Institute of Zoology, CAS, Beijing, focuses on the ecology of endangered Chinese pheasants. YF Zheng was a master student in the IoZ. FW Wei collaborates on this project and he uses macro- and micro-ecological methods to study population biology of mammals in China. XJ Zhan and MW Bruford are molecular ecologists in Cardiff University, where MWB's laboratory focuses on the population genetics and adaptive evolution of endangered and fragmented populations.

Data accessibility

Sampling location and GenBank accession number for each sample are listed in Table S9 (Supporting information).

Supporting information

Additional supporting information may be found in the online version of this article.

Data S1 Methods.

Data S2 Results.

Table S1 Samples of the blood pheasants used in this study and the probability of being the population of origin (MRCA, most recent common ancestor) of different population groups.

Table S2 PCR and internal sequence primers (the last four) used in this study.

Table S3 Survival rate (*s*) of eight galliformes species.

Table S4 Summary of haplotype diversities (*Hd*), nucleotide diversity (π), Tajima's *D* and Fu's (*Fs*), Chakraborty's expected number of alleles, and inferred parameters of population expansion for mitochondrial DNA sequences in the population groups of the blood pheasant.

Table S5 The results of SAMOVA for groupings of populations based on *cyt b + cr* sequences; pops, populations.

Table S6 Parameters of population demography in the blood pheasant: TMRCA, the most recent coalescent ancestor; *N*ef, effective population size; *Theta-W*, the mutation parameter.

Table S7 Morphological differences among the population groups of the blood pheasant inferred from molecular analyses in this study.

Table S8 Pariwise genetic distances (F_{ST}: below diagonal; *Phi*: above diagonal) between the population groups.

Table S9 Sampling location and GenBank accession number for each sample.

Fig. S1 Pariwise genetic distances based on *cyt b* vs. *cyt b + cr* sequences.

Fig. S2 Blood pheasant samples used for the nuclear DNA analysis in this study.

Fig. S3 The maximum likelihood tree based on *cyt b + cr* haplotypes of studied blood pheasants.

Fig. S4 ML phylogenetic trees constructed from nuclear haplotype of ENS00132 (A), ENS13380 (B), ENS01580 (C) and *MC1R* (D), respectively.

Fig. S5 The networks constructed from phased haplotypes of nuclear ENS00132 (A), 13380 (B), 01580 (C) and MC1R (D) sequences of the blood pheasants.

Fig. S6 The PCA result of mtDNA sequences of studied blood pheasants.

Fig. S7 Mismatch distribtution of four population groups of the blood pheasant.

Please note: Wiley-Blackwell are not responsible for the content or functionality of any supporting information supplied by the authors. Any queries (other than missing material) should be directed to the corresponding author for the article.